JOURNAL OF THERMOPHYSICS AND HEAT TRANSFER
Vol. 21, No. 4, October–December 2007

Estimating the Thermal Conductivity of a Film on a Known Substrate

Robert L. McMasters*
Virginia Military Institute, Lexington, Virginia 24450
Ralph B. Dinwiddie†
Oak Ridge National Laboratory, Oak Ridge, Tennessee 37831
and
A. Haji-Sheikh‡
University of Texas at Arlington, Arlington, Texas 76019

DOI: 10.2514/1.25854

Estimating the thermal conductivity of a film on a substrate of known thermal properties is examined in this research. The laser flash method, commonly used in the measurement of thermal diffusivity, is applied to a composite sample, which has a film deposited on a substrate. The laser flash is applied to the substrate and subsequent temperature measurements are recorded from the film side of the sample. Both the thermal conductivity and the volumetric heat capacity of the substrate must be known. Additionally, the volumetric heat capacity of the film must be known. The parameter estimation method used includes nonlinear regression of a transient conduction model in the solid material, which includes allowance for convective heat losses. The thermal conductivity is estimated simultaneously with the magnitude of the flash and the convection coefficient. The direct solution model is a two-layer exact solution which brings about very rapid computation, in contrast to numerical solutions. Several experiments are analyzed, with samples having various values of thermal conductivity, demonstrating the range over which the method can be used.

Nomenclature

$A_n\ B_n\ C_n\ D_n$	=	constants in the series solution, K
a	=	thickness of substrate, m
Bi_1	=	Biot number for the substrate
Bi_2	=	Biot number for the film
b	=	thickness of film, m
c	=	total sample thickness, m
c_{p1}	=	specific heat of the substrate, kJ/kg K
c_{p2}	=	specific heat of the film, kJ/kg K
$G_{i,j}$	=	Green's function, m^{-1}
g	=	internal energy generation, W/m^3
h	=	convection coefficient, $W/m^2 \cdot K$
k_1	=	thermal conductivity of the substrate, $W/m \cdot K$
k_2	=	thermal conductivity of the film, $W/m \cdot K$
L	=	material thickness, m
N	=	norm for the series solution
q_o	=	heat pulse magnitude, J/m^2
S	=	surface area variable for a boundary surface, m^2
T_1	=	temperature of the substrate, K
T_2	=	temperature of the film, K
T_∞	=	ambient temperature, K
t	=	time, s
t^*	=	dimensionless time
V	=	volume, m^3
X_1	=	eigenfunctions for the substrate, K
X_2	=	eigenfunctions for the film, K
x	=	spatial variable in direction of heat transfer, m
x'	=	dummy spatial variable of integration, m
Y_i	=	experimentally measured temperature at time step i, K
α_1	=	substrate thermal diffusivity, m^2/s
α_2	=	film thermal diffusivity, m^2/s
β	=	sensitivity coefficient
γ	=	eigenvalue for substrate, m^{-1}
δ	=	Dirac delta function, s^{-1}
η	=	eigenvalue for film, m^{-1}
λ	=	generic eigenvalue
ρ_1	=	density of substrate, kg/m^3
ρ_2	=	density of film, kg/m^3
σ	=	standard deviation of measurement errors, K
τ	=	dummy variable of integration for time, s
ϕ	=	cross-sectional area of sample, m^2

Presented as Paper 3430 at the 9th AIAA/ASME Joint Thermophysics and Heat Transfer Conference, San Francisco, California, 5–8 June 2006; received 13 June 2006; revision received 7 April 2007; accepted for publication 1 June 2007.

*Department of Mechanical Engineering, Virginia Military Institute, Lexington, VA 24450. AIAA Member.
†High Temperature Materials Laboratory, Oak Ridge National Laboratory, Oak Ridge, TN 37831.
‡Department of Mechanical and Aerospace Engineering, University of Texas at Arlington, Arlington, TX 76019.

I. Introduction

THERMAL diffusivity has been measured using the flash method for several decades [1,2]. Flash diffusivity measurement has become common over this period of time and several companies make flash diffusivity instruments. Using this method, a small disc-shaped sample of material, usually 1–2 cm in diameter with a thickness of 1–2 mm, is placed in the flash diffusivity instrument. The sample is then subjected to a brief but intense laser flash with a duration of several milliseconds and an intensity of several kilowatts per square millimeter. Temperature measurements are recorded on the nonheated side of the sample as a function of time, usually with an optical measurement system. The temperature recordings are then analyzed to determine the thermal diffusivity of the material. The flash diffusivity method has the advantages of requiring only a small sample and experiments can be conducted in a short amount of time, with experiment durations on the order of seconds. Additionally, the noncontact temperature measurement system allows samples to be tested at very high temperatures.

The research described in this paper involves the analysis of flash heating experiments where a sample consisting of two layers is to be analyzed. In the classical flash diffusivity experiments performed historically, only thermal diffusivity was calculated from the experimental results. Maillet et al. [3] addressed coatings on flash diffusivity experiments by allowing for a time shift in the temperature measurement. The area of interest in this work was to find the thermal diffusivity of the substrate rather than the film. From this, of course, thermal conductivity can be calculated if volumetric heat capacity is known. In the present research, the parameter of interest is the thermal conductivity of the film coating, which is bonded to the sample substrate. Because only thermal diffusivity can be obtained through flash diffusivity experiments, the following parameters must be known to obtain the desired results: substrate thermal conductivity, substrate volumetric heat capacity, substrate thickness, film thickness, and film volumetric heat capacity.

During the flash heating test, the substrate is subjected to a nearly instantaneous heat addition imparted from a laser. The surface temperature on the opposite side of the material is then recorded as a function of time and placed in a computer data file. Based on the analysis of this data, the following three parameters are estimated, by software developed as part of this research, using a nonlinear regression procedure: 1) film thermal conductivity, 2) thermal convection coefficient, and 3) magnitude of heat absorbed during the flash.

The program provides graphical and tabular output of the results. Additionally, the user can make several selections as to how the parameters are computed, including selections on convergence criteria and the number of iterations allowed in attempting to obtain convergence.

II. Direct Solution

In any parameter estimation procedure, a direct solution is required which models the physical process. In the present research, an analytical solution is used as opposed to a numerical solution, primarily due to the speed with which an analytical solution can be computed. The higher accuracy attainable with analytical solutions is an additional benefit. Multilayer exact solutions were discussed by de Monte [4]. This is contrasted to the method used by Aviles-Ramos and Haji-Sheikh [5] which followed a Green's function approach. Likewise, the present research uses Green's functions, but is subjected to flash heating and involves isotropic materials. See Fig. 1 for the experimental configuration used in the present research.

Two differential equations are considered for the direct solution in this work, one for each of the material layers. Specifically, these equations are

$$k_1 \frac{\partial^2 T_1}{\partial x^2} = \rho_1 c_{p1} \frac{\partial T_1}{\partial t} \quad \text{and} \quad k_2 \frac{\partial^2 T_2}{\partial x^2} = \rho_2 c_{p2} \frac{\partial T_2}{\partial t} \tag{1}$$

The boundary conditions for this problem are

$$\begin{aligned} -k_1 \frac{\partial T_1}{\partial x}\bigg|_{x=0} &= h(T_\infty - T_1) + q_o \delta(t) \quad \text{and} \\ -k_2 \frac{\partial T_2}{\partial x}\bigg|_{x=c} &= h(T_2 - T_\infty) \end{aligned} \tag{2}$$

and the compatibility conditions at $x = a$ are

$$T_1 = T_2 \quad \text{and} \quad k_1 \frac{\partial T_1}{\partial x}\bigg|_{x=a} = k_2 \frac{\partial T_2}{\partial x}\bigg|_{x=a} \tag{3}$$

The initial conditions for this problem are

$$T_1(x,0) = T_2(x,0) = T_\infty \tag{4}$$

As can be seen here, the convection coefficients on both sides of the sample are assumed to be equivalent. This is normally the case in flash diffusivity experiments because of the low temperature rises of only a few degrees Celsius, which are features designed into the laboratory instruments. The goal is to have the experiment conducted as close to isothermally as possible. Using separation of variables to solve these equations results in two sets of eigenvalues, one for each material. These eigenvalues are defined as

$$\frac{X_1''}{X_1} = -\frac{\lambda^2}{\alpha_1} = -\gamma^2 \tag{5}$$

and

$$\frac{X_2''}{X_2} = -\frac{\lambda^2}{\alpha_2} = -\eta^2 \tag{6}$$

where $\alpha_1 = k_1/\rho_1 c_{p1}$ and $\alpha_2 = k_2/\rho_2 c_{p2}$. The temperature solutions T_1 and T_2 take the following forms

$$T_1 = \sum_{n=1}^{\infty} X_{1,n}(\gamma_n x) \exp(-\lambda_n^2 t) \tag{7}$$

$$T_2 = \sum_{n=1}^{\infty} X_{2,n}(\eta_n x) \exp(-\lambda_n^2 t) \tag{8}$$

where

$$X_{1,n}(\gamma_n x) = A_n \cos(\gamma_n x) + B_n \sin(\gamma_n x) \tag{9}$$

and

$$X_{2,n}(\eta_n x) = C_n \cos(\eta_n x) + D_n \sin(\eta_n x) \tag{10}$$

To provide a complete solution, the constants A_n, B_n, C_n, and D_n must be obtained, as well as the eigenvalues γ_n and η_n. As a starting point, we will satisfy the boundary condition

$$k_1 \frac{\partial X_1}{\partial x}\bigg|_{x=0} = h X_1|_{x=0} \tag{11}$$

After substituting for X_1 and $\partial X_1/\partial x$, and dropping the n index subscripts for convenience, this boundary condition becomes

$$k_1[-A\gamma \sin(\gamma x) + B\gamma \cos(\gamma x)]_{x=0} = h[A \cos(\gamma x) + B \sin(\gamma x)]_{x=0} \tag{12}$$

or $k_1 B\gamma = hA$ which reduces to

$$A = \frac{k_1 B \gamma}{h} \tag{13}$$

Next, the compatibility conditions at $x = a$, must be satisfied, as given in Eq. (3). With the elimination of the constant A, the eigenfunction X_1 can now be expressed as

$$X_1 = \frac{k_1 B\gamma}{h}\cos(\gamma x) + B \sin(\gamma x) = B\left[\frac{k_1 \gamma}{h}\cos(\gamma x) + \sin(\gamma x)\right] \tag{14}$$

and $\partial X_1/\partial x$ is

$$\frac{\partial X_1}{\partial x} = B\gamma\left[-\frac{k_1 \gamma}{h}\sin(\gamma x) + \cos(\gamma x)\right] \tag{15}$$

Substituting these expressions into the compatibility condition, Eq. (3), for temperature we have

$$B\left[\frac{k_1 \gamma}{h}\cos(\gamma a) + \sin(\gamma a)\right] = C \cos(\eta a) + D \sin(\eta a) \tag{16}$$

and for the heat flux condition we have

$$\begin{aligned} &k_1 B\gamma\left[-\frac{k_1 \gamma}{h}\sin(\gamma a) + \cos(\gamma a)\right] \\ &\quad = k_2[-C\eta \sin(\eta a) + D\eta \cos(\eta a)] \end{aligned} \tag{17}$$

Rearranging these equations, we have

$$\left(\frac{C}{B}\right)\cos(\eta a)+\left(\frac{D}{B}\right)\sin(\eta a)$$
$$=\left[\frac{k_1\gamma}{h}\cos(\gamma a)+\sin(\gamma a)\right]-\left(\frac{C}{B}\right)\sin(\eta a)+\left(\frac{D}{B}\right)\cos(\eta a)$$
$$=\left(\frac{k_1}{k_2}\right)\left(\frac{\gamma}{\eta}\right)\left[-\frac{k_1\gamma}{h}\sin(\gamma a)+\cos(\gamma a)\right] \tag{18}$$

At this point, these two equations can be solved for the two constants C/B and D/B. These ratios are

$$\frac{C}{B}=\left[\frac{k_1\gamma}{h}\cos(\gamma a)\cos(\eta a)+\sin(\gamma a)\cos(\eta a)\right]$$
$$+\left(\frac{\gamma k_1}{\eta k_2}\right)\left[\frac{k_1\gamma}{h}\sin(\gamma a)\sin(\eta a)-\cos(\gamma a)\sin(\eta a)\right] \tag{19}$$

and

$$\frac{D}{B}=\left[\frac{k_1\gamma}{h}\cos(\gamma a)\sin(\eta a)+\sin(\gamma a)\sin(\eta a)\right]$$
$$-\left(\frac{\gamma k_1}{\eta k_2}\right)\left[\frac{k_1\gamma}{h}\sin(\gamma a)\cos(\eta a)-\cos(\gamma a)\cos(\eta a)\right] \tag{20}$$

We now have expressions for the constants A/B, C/B, and D/B so that we can express the solutions in the two regions as

$$T_1(x,t)=\sum_{n=1}^{\infty}Be^{-\lambda_n^2 t}\left(\frac{k_1\gamma}{h}\cos\gamma x+\sin\gamma x\right) \tag{21}$$

and

$$T_2(x,t)=\sum_{n=1}^{\infty}Be^{-\lambda_n^2 t}\left(\frac{C}{B}\cos\eta x+\frac{D}{B}\sin\eta x\right) \tag{22}$$

where C/B and D/B are long expressions, defined by Eqs. (19) and (20), but constants nevertheless. We now have only one unknown constant, namely B, which we can eliminate if we apply the initial condition.

$$T_1(x,0)=\sum_{n=1}^{\infty}B\left(\frac{k_1\gamma}{h}\cos\gamma x+\sin\gamma x\right)=T_\infty \tag{23}$$

for the left side of the material and

$$T_2(x,0)=\sum_{n=1}^{\infty}B\left(\frac{C}{B}\cos\eta x+\frac{C}{B}\sin\eta x\right)=T_\infty \tag{24}$$

If we multiply both sides by the eigenfunction and integrate over the whole domain, adding both equations together, we have

$$\int_0^b\sum_{n=1}^{\infty}B\left(\frac{k_1\gamma}{h}\cos\gamma x+\sin\gamma x\right)\left(\frac{k_1\gamma_m}{h}\cos\gamma_m x+\sin\gamma_m x\right)\mathrm{d}x$$
$$+\int_b^c\sum_{n=1}^{\infty}B\left(\frac{C}{B}\cos\eta x+\frac{D}{B}\sin\eta x\right)\left(\frac{C}{B}\cos\eta_m x+\frac{D}{B}\sin\eta_m x\right)\mathrm{d}x$$
$$=\int_0^b T_\infty\left(\frac{k_1\gamma_m}{h}\cos\gamma_m x+\sin\gamma_m x\right)\mathrm{d}x$$
$$+\int_b^c T_\infty\left(\frac{C}{B}\cos\eta_m x+\frac{D}{B}\sin\eta_m x\right)\mathrm{d}x \tag{25}$$

The principle of orthogonality can now be applied, which causes each term on the left-hand side to be zero, whenever the subscript m does not equal n.

$$\int_0^b B\left(\frac{k_1}{h}\cos\gamma x+\sin\gamma x\right)^2\mathrm{d}x+\int_b^c B\left(\frac{C}{B}\cos\eta x+\frac{D}{B}\sin\eta x\right)^2\mathrm{d}x$$
$$=\int_0^b T_\infty\left(\frac{k_1}{h}\cos\gamma x+\sin\gamma x\right)\mathrm{d}x$$
$$+\int_b^c T_\infty\left(\frac{C}{B}\cos\eta x+\frac{D}{B}\sin\eta x\right)\mathrm{d}x \tag{26}$$

The left-hand side of this equation is typically defined as the norm, which we represent with the symbol N. Because the constant B is defined arbitrarily, we can write

$$BN=\int_0^b B\left(\frac{k_1}{h}\cos\gamma x+\sin\gamma x\right)^2\mathrm{d}x$$
$$+\int_b^c B\left(\frac{C}{B}\cos\eta x+\frac{D}{B}\sin\eta x\right)^2\mathrm{d}x \tag{27}$$

Alternatively, we can lump the arbitrary constant B into the norm by setting its value equal to one and we have

$$N=\int_0^b\left(\frac{k_1}{h}\cos\gamma x+\sin\gamma x\right)^2\mathrm{d}x+\int_b^c(C\cos\eta x+D\sin\eta x)^2\,\mathrm{d}x \tag{28}$$

With the norm defined this way, the solution can be cast in the form of a Green's function. In general, for all boundary conditions, the Green's function is

$$G_{ij}(x,t|x',\tau)=\sum_{n=0}^{\infty}\frac{\rho_j c_{pj}X_{i,n}(x)X_{j,n}(x')}{N_n}\exp[-\lambda_n^2(t-\tau)] \tag{29}$$

where $i=1,2$ and $j=1,2$ corresponding to the regions in the body. In this formulation, the eigenfunction $X_{i,n}(x)$ corresponds to the region in which the temperature is to be computed and the eigenfunction $X_{j,n}(x')$ corresponds to the region in which the boundary condition, initial condition, or internal energy generation takes place. These eigenfunctions are given in general form in Eqs. (9) and (10).

The general Green's function solution equation, as given in Beck et al. [6], for region i is

$$T_i(x,t)=\sum_{j=1}^{2}\int_{V_j}G_{ij}(x,t|x',0)T_j(x',0)\,\mathrm{d}V_j'$$
$$+\sum_{j=1}^{2}\int_{\tau=0}^{t}\int_{V_j}\frac{1}{\rho_j c_{pj}}G_{ij}(x,t|x',\tau)g_j(x',\tau)\,\mathrm{d}V_j'\,\mathrm{d}\tau$$
$$+\sum_{j=1}^{2}\int_{\tau=0}^{\tau=t}\int_{S_j}\frac{k_j}{\rho_j c_{pj}}\left[G_{ij}(x,t|x',\tau)\frac{\partial T(x',\tau)}{\partial x}\right.$$
$$\left.-T(x',\tau)\frac{\partial G_{ij}(x,t|x',\tau)}{\partial x}\right]_{S_j}\mathrm{d}S_j\,\mathrm{d}\tau \tag{30}$$

In this formulation, S is the surface area at each of the boundaries. This equation is made up of three salient terms. Each term is a summation from 1 to 2, because this corresponds to the number of regions in the body. Of the three main terms in this equation, the first term accounts for the initial conditions, the second term deals with internal heat generation, and the last term handles nonhomogeneous boundary conditions. In the present case, the initial conditions throughout both regions are ambient temperature, allowing us to neglect the first term. Because there is no internal energy generation, the second term can be neglected as well. Finally, the only nonhomogeneous boundary condition is the flash heating, which takes place only at time $t=0$ and $x=0$. Moreover, the flash heating in all flash diffusivity measurement formulations is considered to be uniform over the surface, eliminating the need to perform the surface integration. For these reasons, the final integration is simply the

Green's function evaluated at the $x = 0$ boundary, multiplied by the magnitude of the heat flux at the surface.

The location for temperature measurements in the flash heating experiment is at the right-hand surface, that is, the film exterior surface. Therefore, we are interested only in the temperature solution for region 2. Of course, the equations for both regions have to be solved simultaneously to obtain the solution for the second half of the body. When evaluating the Green's function at the instant of the flash ($t = 0$), the X_2 portion of the solution remains a function of x and the X_1 solution is a function of x', which is then evaluated at $x' = 0$. This simplifies the temperature solution in the second region to

$$T_2(x,t) = -\int_{\tau=0}^{\tau=t} \frac{k_1}{\rho_1 c_{p1}} G_{ij}(x,t|x',\tau) \frac{\partial T_1(x',\tau)}{\partial x} \phi \, \mathrm{d}\tau \tag{31}$$

where ϕ represents the cross-sectional area perpendicular to the direction of the heat flux which comes from integrating over the surface. Also, the flash heating can be expressed as

$$q\delta(\tau) = -k_1 \frac{\partial T_1(x',\tau)}{\partial x} \tag{32}$$

Substituting this into the integral, we have

$$T_2(x,t) = \frac{\phi}{\rho_1 c_{p1}} \int_{\tau=0}^{\tau=t} G_{ij}(x,t|x',\tau) q\delta(\tau) \, \mathrm{d}\tau \tag{33}$$

Substituting the Green's function, the solution becomes

$$T_2(x,t) = \frac{\phi}{\rho_1 c_{p1}} \int_{\tau=0}^{\tau=t} \sum_{n=0}^{\infty} \frac{\rho_1 c_{p1} X_{2,n}(x) X_{1,n}(x')}{N_n} \times \exp[-\lambda_n^2 (t-\tau)] q_o \delta(\tau) \, \mathrm{d}\tau \tag{34}$$

Now the $\rho_1 c_{p1}$ terms cancel and the eigenfunctions can be evaluated at their respective values of $x = c$ and $x' = 0$. When this is done, the solution becomes

$$T_2(c,t) = \phi q_o \int_{\tau=0}^{\tau=t} \sum_{n=0}^{\infty} \frac{A(C\cos\eta c + D\sin\eta c)}{N_n} \times \exp[-\lambda_n^2 (t-\tau)] \delta(\tau) \, \mathrm{d}\tau \tag{35}$$

Finally, performing the integration, we have

$$T_2(c,t) = \phi q \sum_{n=1}^{\infty} \frac{A(C\cos\eta c + D\sin\eta c)}{N_n} e^{-\lambda_n^2 t} \tag{36}$$

In evaluating the norm N_n using Eq. (28), we have the general definition

$$N_n = \sum_{j=1}^{M} \int_{V_j} \rho_j c_{pj} [X_{j,n}(x')]^2 \, \mathrm{d}V_j' \tag{37}$$

In the specific case of the two-layer problem at hand, once again dropping the subscript index for convenience, this becomes

$$N = \int_0^a \rho_1 c_{p1} (A\cos\gamma x + \sin\gamma x)^2 \, \mathrm{d}x + \int_a^c \rho_2 c_{p2} (C\cos\eta x + D\sin\eta x)^2 \, \mathrm{d}x \tag{38}$$

Performing the integration, we have

$$\begin{aligned} N = {} & \rho_1 c_{p1} \left[A^2 \left(\frac{a}{2} + \frac{1}{4\gamma} \sin 2\gamma a \right) + \frac{A}{\gamma} \sin^2 \gamma a \right. \\ & \left. + \left(\frac{a}{2} - \frac{1}{4\gamma} \sin 2\gamma a \right) \right] \\ & + \rho_2 c_{p2} C^2 \left(\frac{b}{2} + \frac{1}{4\eta} (\sin 2\eta c - \sin 2\eta a) \right) \\ & + \rho_2 c_{p2} \frac{CD}{\eta} (\sin^2 \eta c - \sin^2 \eta a) \\ & + D^2 \left(\frac{b}{2} - \frac{1}{4\eta} (\sin 2\eta c - \sin 2\eta a) \right) \end{aligned} \tag{39}$$

Finally, the eigenvalues are computed by applying the boundary condition at $x = c$ as given by Eq. (2)

$$-k_2 \left. \frac{\partial X_2}{\partial x} \right|_{x=c} = h X_2|_{x=c} \tag{40}$$

Applying this boundary condition, we have

$$C\left[\sin(\eta c) - \frac{h}{k_2 \eta} \cos(\eta c) \right] - D\left[\cos(\eta c) + \frac{h}{k_2 \eta} \sin(\eta c) \right] = 0 \tag{41}$$

Substituting the values for C and D as found in Eqs. (19) and (20), this equation can be reduced to the eigencondition

$$\frac{\eta b \tan(\eta b) - Bi_2}{Bi_2 \tan(\eta b) + \eta b} = -\left(\frac{\gamma k_1}{\eta k_2} \right) \frac{\gamma a \tan(\gamma a) - Bi_1}{Bi_1 \tan(\gamma a) + \gamma a} \tag{42}$$

where $Bi_1 = ha/k_1$ and $Bi_2 = hb/k_2$. Because two sets of eigenvalues are being computed simultaneously, the process of finding the roots of the eigencondition must include consideration of both sets of eigenvalues. The roots of the eigencondition will lie between asymptotes which occur at highly irregular intervals. Asymptotes of this equation occur at $Bi_2 \tan(\eta b) + \eta b = 0$ and at $Bi_1 \tan(\gamma a) + \gamma a = 0$ which cause the eigenequation to reach infinity. Therefore, the values for η and γ which satisfy the preceding two equations serve as values between which eigenvalues exist.

Finding these asymptotes is very important because some of them are very close together and others are quite far apart. Unless the locations of the asymptotes are known, it would be nearly impossible to avoid missing some of the eigenvalues. Once these asymptotes are located, the eigenvalues can be found by searching directly between each pair of asymptotes using Newton's method to find the roots of the eigencondition [7].

III. Parameter Estimation

With the direct solution in place, the parameter estimation aspect of the problem can be undertaken. It is desirable to solve for the minimum number of parameters necessary. This facilitates the greatest degree of stability in the parameter estimation procedure and the greatest degree of confidence in the calculated parameters. The unknown parameters for this model are thermal conductivity of the film k_2, heat transfer coefficient h, and the incident heat flux absorbed q_0. To find the parameters, the method of least squares is used as outlined in Beck and Arnold [8]. The method of least squares minimizes the following expression

$$S = \sum_{i=1}^{n} (Y_i - T_i)^2 \tag{43}$$

where Y_i represents the temperature measurements and T_i represents the calculated temperatures from the model described in the direct solution development.

To minimize this expression, aside from using trial and error, the sensitivity coefficients must first be calculated. This is accomplished by taking partial derivatives of the direct temperature solution with respect to each of the parameters, one at a time. The sensitivity

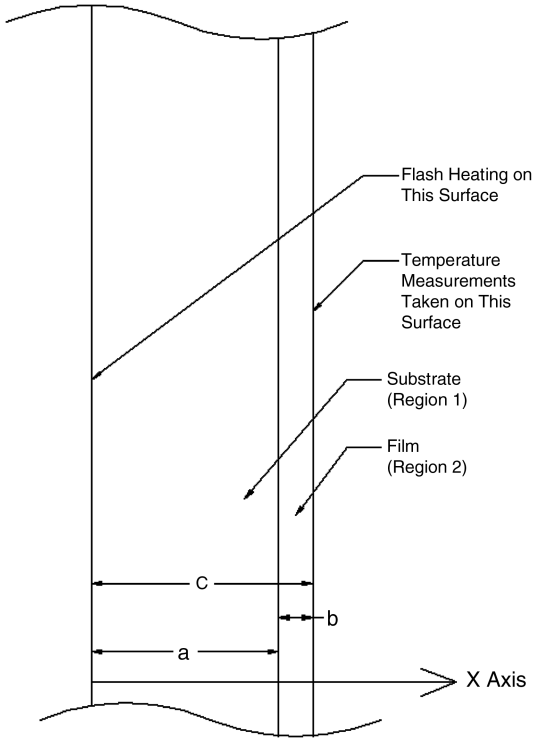

Fig. 1 Sample configuration in experiment.

coefficients are then normalized by multiplying by the respective parameter. In this way, the units of the sensitivity coefficients are always in temperature and the magnitudes of the coefficients are directly comparable. For example, the sensitivity coefficient for k_2, the first parameter of interest in the model discussed in the preceding paragraph, is

$$\beta_1 = k_2 \frac{\partial T}{\partial k_2} \tag{44}$$

Using these sensitivity coefficients, a set of matrix equations can be developed and solved using the method of least squares. The parameter estimates must be found iteratively because the sensitivity coefficients for this problem are nonlinear. There will be three such sensitivity coefficients for this analysis, one for each unknown parameter. A graph of the sensitivity coefficients for this model, expressed as functions of time, is shown in Fig. 2. The parameters for the direct solution, from which the plotted sensitivity coefficients were taken, are from a test case using the following parameters:

Substrate thermal conductivity k_1: 1.0 $\mathrm{W/m \cdot K}$
Substrate volumetric heat capacity $\rho_1 c_1$: 10^6 $\mathrm{J/m^3 \cdot K}$
Substrate thickness a: 0.8 mm
Film thickness b: 0.2 mm
Film volumetric heat capacity $\rho_2 c_2$: 10^6 $\mathrm{J/m^3 \cdot K}$
Film thermal conductivity k_2: 0.01 $\mathrm{W/m \cdot K}$
Convection coefficient h: 20 $\mathrm{W/m^2 \cdot K}$
Magnitude of heat absorbed during the flash q_o: 1000 $\mathrm{J/m^2}$

The nature of the flash experiments is such that the sensitivity coefficients for the heat flux parameter and the convection coefficient parameter are somewhat correlated, an undesirable condition. This is evidenced by the similar shape of the two sensitivity coefficient curves. The sensitivity coefficient curve for thermal conductivity, however, has a slightly different shape than the others, which makes it a more salient parameter. When sensitivity curves are correlated, the individual parameters become difficult to distinguish between one another and the parameter estimation algorithm is not as robust. The thermal conductivity sensitivity coefficient is distinguishable enough from the other curves in the experiment depicted in Fig. 2, that convergence is obtainable in this test case.

Figure 3 shows the same three sensitivity coefficients plotted for a different experiment with the only difference being that it is based on a larger film conductivity by a factor of 20. Notice the shorter duration of the transients in this experiment in comparison to that in Fig. 2. This is because the higher thermal conductivity allows the thermal conduction to take place more quickly. Notice also that the peak value for the thermal conductivity sensitivity coefficient of approximately 0.25 K is substantially less than the corresponding value of 0.4 K in Fig. 2. This means that convergence should be easier to obtain from the experiment depicted in Fig. 2 because the thermal conductivity sensitivity coefficient is larger than in the Fig. 3 case.

It is desirable to develop a systematized way of categorizing experiments to determine optimum experimental design, or at least an indication as to whether film thermal conductivity can be determined at all in certain experiments. Pursuant to this goal, a matrix of synthetic experiments was generated to determine the maximum value of the film thermal conductivity sensitivity coefficient under various combinations of film thicknesses and thermal conductivities. Figure 4 shows a plot summarizing the results of these tests. In each of the tests, the overall sample thickness was held at 1 mm and only the film thickness and film thermal conductivity were allowed to vary. All other parameters were held at the values noted previously. As can be seen in this figure, the largest peak in the sensitivity coefficient for thermal conductivity comes at a higher value of film thermal conductivity as the thickness of the film increases. This seems to be a logical trend, because the primary means of discrimination between the film and the substrate is rooted in a delay of the thermal "wave" penetrating through the material during the experiment. As can be seen on this plot, for cases where there is a thin film with a high thermal conductivity, the peak sensitivity coefficient for film thermal conductivity is extremely low. This bodes poorly for obtaining convergence in an experiment under these conditions. Conversely, with a relatively thick film having a low thermal conductivity, the sensitivity coefficient for film thermal conductivity is much larger, which greatly increases the probability of convergence in the parameter estimation program.

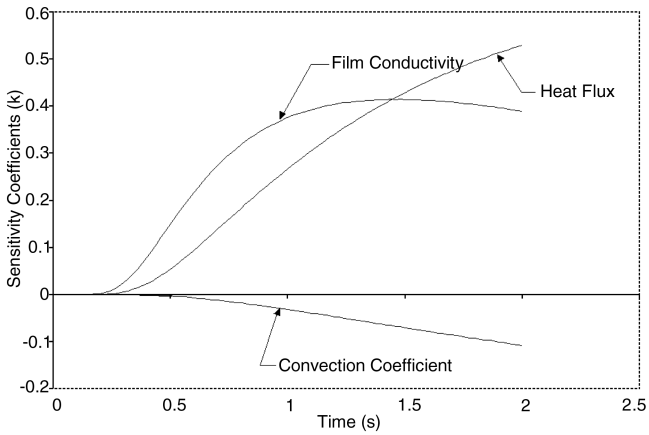

Fig. 2 Plot of the three sensitivity coefficients for a test experiment (q_o, k_2, h), with a conductivity of 0.01 $\mathrm{W/m \cdot K}$.

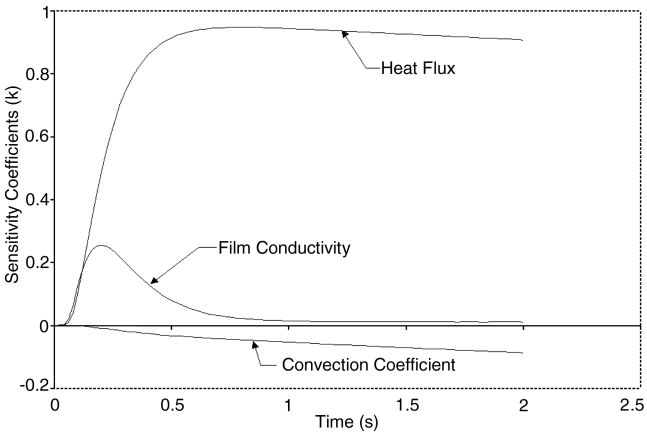

Fig. 3 Plot of the three sensitivity coefficients for a test experiment (q_o, k_2, h) from top to bottom, with a conductivity of 0.2 $\mathrm{W/m \cdot K}$.

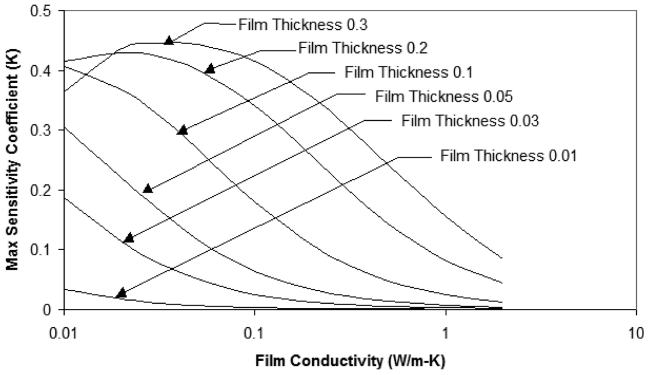

Fig. 4 Plot of the peak value of thermal conductivity sensitivity coefficient $k_2 \partial T/\partial k_2$ as a function of film conductivity k_2 for various film thicknesses (in millimeters).

The trend toward a higher peak sensitivity coefficient for thick films of low conductivity has a limit, as can be seen in Fig. 4 as well. When the film becomes extremely thick with a low thermal conductivity, the duration of time required for the thermal wave to transmit through the sample is increased. As a result, surface heat losses have more time to act and the peak temperature reached on the film side of the sample is lower. This effectively decreases the peak of the sensitivity coefficient plot for film thermal conductivity. Figure 4 simply plots the peak value reached by the sensitivity coefficient for thermal conductivity at any time using the corresponding parameters. Note that the peak value of 0.4 reached by this sensitivity coefficient in Fig. 3 corresponds to the same 0.4 value in Fig. 4 when using the same 0.2 mm film thickness and a film conductivity of 0.05 $\mathrm{W/m \cdot K}$ on a 0.8 mm substrate.

To obtain more insight into the optimal design of the experiment, the same data plotted on Fig. 4 were replotted in Fig. 5 in a different format. The objective of the design of the experiment is to establish the experimental parameters necessary to obtain the greatest sensitivity to the parameter of interest. In this case, film and substrate thicknesses and thermal conductivities should be selected to obtain the largest possible peak in the sensitivity coefficient curve for film thermal conductivity. Attention must also be given to ensuring the sensitivity coefficient curves are somewhat uncorrelated. To help accomplish this, the concept of "diffusion thickness ratio" was developed as part of this research. This concept is based on the principle of dimensionless time in thermal conduction, which is normally expressed as

$$t^* = \frac{\alpha t}{L^2} \tag{45}$$

Using the fact that the majority of a thermal transient in conduction is completed at a dimensionless time of one, if we set t^* to this value, we find that the time required for this transient to take place is

$$t = \frac{L^2}{\alpha} \tag{46}$$

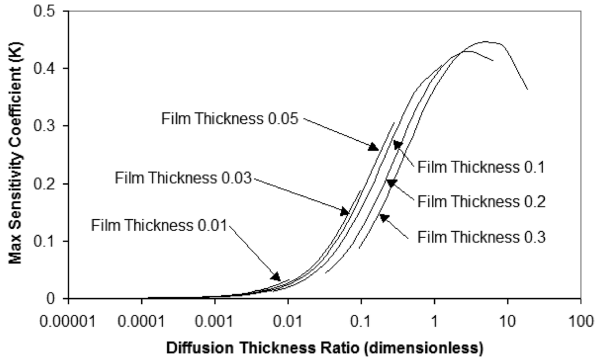

Fig. 5 Plotting the same information as in Fig. 4 with respect to the dimensionless "diffusion thickness ratio" $b^2\alpha_1/a^2\alpha_2$.

where L is the generic thickness of a piece of material. Although this term carries units of time, it is referred to here as the "diffusion thickness" because this gives a feel for the effective penetration time required for the thermal wave. More time required for penetration equates to a more "thick" sample. If we then examine the ratio of the diffusion thicknesses of the film and the substrate, we have a rough idea of the amount of time it will take for diffusion to take place in the film as compared to the substrate. The ratio of these diffusion thicknesses can be written as

$$\text{Diffusion Thickness Ratio} = \frac{L_2^2 \alpha_1}{L_1^2 \alpha_2} \tag{47}$$

Plotting the peak thermal conductivity sensitivity coefficient against this diffusion thickness ratio, we find that there is a definite correlation between the two, regardless of film thickness or film thermal conductivity. Figure 5 now provides a convenient tool to use in the design of experiments involving the determination of film thermal conductivity in flash diffusivity tests.

To make effective use of Fig. 5, it would be useful to know the likelihood of convergence associated with various values of the maximum sensitivity coefficient for the thermal conductivity of the film. To determine this, synthetic experiments were generated using the program developed as part of this research in the "direct solution" mode. For this set of experiments, the same parameters were used as in the preceding figures with the film thickness maintained at 0.1 mm. The film conductivity varied between 0.03 and 0.5 $\mathrm{W/m \cdot K}$. Next, these experiments were analyzed using the program in "parameter estimation" mode. Additionally, errors with a Gaussian distribution were impressed on two sets of the synthetic experiments to simulate experimental measurement errors. One set of errors had a standard deviation of $\sigma = 0.30$°C and the other was $\sigma = 0.45$°C. This is significant in that, with the parameter values used in this example, the peak temperature in the sample was less than 1°C. Therefore, the impressed error values were very large with respect to the measurements.

With all nonlinear parameter estimation, initial values for the unknown parameters must be provided as input data to begin the nonlinear regression process. If the initial values are significantly different from those of the true parameter values, convergence is more difficult to obtain. Figure 6 shows a plot of the maximum value of the error in the initial parameter values selected, which still allowed convergence for various values of peak sensitivity coefficient for film thermal conductivity. This plot essentially gives a picture of the robustness of the parameter estimation method, under different experimental conditions. Note that, if the peak sensitivity coefficient was less than 0.1°C, convergence could not be obtained unless employing error-free data. Otherwise, as the peak sensitivity coefficient increased, convergence was still obtainable, even with initial parameter values that were off from the true values by a factor of 10 in some cases. Although adding the impressed errors to the data deteriorated the performance of the parameter estimation method, a fairly large error in the initial parameter values could still bring about

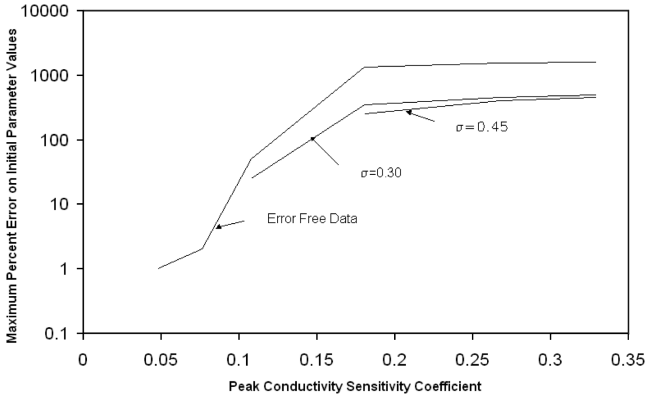

Fig. 6 Likelihood of convergence as a function of peak value for the sensitivity coefficient for film thermal conductivity $k_2 \partial T/\partial k_2$.

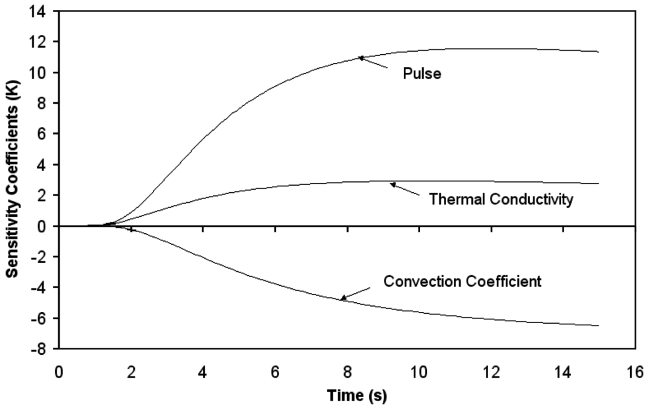

Fig. 7 Sensitivity coefficients for the laboratory sample show correlation between each of the three parameters (q_o, k_2, h), making convergence very difficult.

convergence. However, the threshold for obtaining convergence was higher in terms of the peak value for the film conductivity sensitivity coefficient.

IV. Analysis of Laboratory Data

A two-layer sample with a substrate of epoxy and a film of carbon black was prepared at Michigan State University and tested using the flash diffusivity instrument at the High Temperature Materials Laboratory at Oak Ridge National Laboratory. The intention was to make the conductivity of the film lower than that of the substrate so as to allow effective estimation of the film conductivity. Because the film in this case was extremely thin at 15μm, the thermal conductivity had to be very low to produce an adequately large sensitivity coefficient for estimation of the film thermal conductivity.

The thermal conductivity of the epoxy substrate in this experiment was measured at $0.14\ \mathrm{W/m \cdot K}$ and the volumetric heat capacity was $1,159,000\ \mathrm{J/m^3 \cdot K}$. The volumetric heat capacity of the carbon black was $1,440,000\ \mathrm{J/m^3 \cdot K}$. As stated in the introduction, these properties must be known to estimate the thermal conductivity of the carbon black film. Very little data exists regarding the thermal conductivity of carbon black.[§] Moreover, the conductivity can be highly variable, depending on the structure and porosity of the carbon black, because it is a discontinuous agglomeration of submicron graphite particles. In particular, the samples were analyzed in a vacuum environment during the tests conducted using the Oak Ridge flash diffusivity instrument. This environment causes the lowest possible thermal conductivity to be exhibited by a porous material. As a basis of comparison from the literature, a value of $0.05\ \mathrm{W/m \cdot K}$ was found for thermal conductivity of charcoal dust [9]. At various degrees of vacuum, powders such as pearlite exhibit thermal conductivities ranging from 0.03 to $0.0001\ \mathrm{W/m \cdot K}$, with the lowest thermal conductivity exhibited at the greatest value of vacuum [10].

The data from the experiment involving this two-layer sample, which were measured using the Oak Ridge flash diffusivity instrument, were next analyzed using the computer program developed in this research. The results obtained showed a very low thermal conductivity in the carbon black film. Three tests were run on the same sample. The thinness of the film made the sensitivity coefficient for the thermal conductivity of the film very low. Figure 7 shows the sensitivity coefficients for this experiment. As can be seen from this plot, the three sensitivity coefficients are correlated. More significantly, the sensitivity coefficient for the parameter of interest, thermal conductivity, exhibits the smallest magnitude of the three parameters.

Indeed, convergence was difficult to obtain and the normal convergence criterion, requiring all parameter estimates to change less than 1% between iterations, had to be relaxed to 3% to achieve convergence. Even at this, convergence was only obtainable in two of the three experiments. The values obtained for the thermal conductivity in these two experiments were 0.000783 and $0.000745\ \mathrm{W/m \cdot K}$. The standard deviation of the residuals in these cases was approximately 0.048°C with a maximum temperature rise in the experiment of approximately 13°C. This residual magnitude corresponds to approximately 0.37% of the maximum temperature rise, which indicates that the model follows the measured data quite closely. With the extremely low thermal conductivity found for carbon black, even though the film was very thin, the diffusion thickness ratio for this experiment was approximately 0.011, which was at the low end of the acceptable window for the use of this method. If the data had contained larger measurement errors, convergence would have been unlikely. This corresponds unsurprisingly to the fact that the convergence criteria had to be relaxed from the normal 1% variation in all parameters between iterations to 3% variation between iterations.

V. Conclusions

A method was successfully developed to determine the thermal conductivity of a film on a substrate of known thermal conductivity using the flash diffusivity method. Sensitivity coefficients were used to establish guidelines for the use of this method so as to maximize the sensitivity of the experiment to the thermal conductivity of the film. A range of diffusion thickness ratios was found over which the method would produce results by converging on a solution. Finally, an actual experimental sample was tested in a flash diffusivity instrument and the method was successful in finding the thermal conductivity of the film, even though the conditions of the experiment were at the outer limits of the method's capabilities.

Acknowledgment

Special gratitude is expressed to Hiroyuki Fukishima of Michigan State University for his preparation of the two-layer epoxy/carbon black sample used in the analysis of the empirical measurements as part of this work.

References

[1] Parker, W., Jenkins, Butler, C., and Abbott, G., "Flash Method of Determining Thermal Diffusivity, Heat Capacity and Thermal Conductivity," *Journal of Applied Physics*, Vol. 32, No. 9, 1961, pp. 1679–1684.

[2] Cowan, R., "Pulse Method of Measuring Thermal Diffusivity at High Temperature," *Journal of Applied Physics*, Vol. 34, No. 4, 1963, 926–927.

[3] Maillet, D., Moyne, C., and Remy, B., "Effect of a Thin Layer on the Measurement of Thermal Diffusivity of a Material by the Flash Method," *International Journal of Heat and Mass Transfer*, Vol. 43, 2000, pp. 4057–4060.

[4] de Monte, F., "Transient Heat Conduction in a One-Dimensional Composite Slab: A 'Natural' Analytic Approach," *International Journal of Heat and Mass Transfer*, Vol. 43, 2000, pp. 3607–3619.

[5] Aviles-Ramos, C., and Haji-Sheikh, A., "Estimation of Thermophysical Properties of Composites Using Multi-Parameter Estimation and Zeroth Order Regularization," *Inverse Problems in Engineering*, Vol. 9, No. 5, 2001, pp. 507–536.

[6] Beck, J., Cole, K., Haji-Sheikh, A., and Litkouhi, B., *Heat Conduction Using Green's Functions*, Hemisphere, Washington, D.C., 1992.

[7] Aviles-Ramos, C., Harris, K., and Haji-Sheikh, A., "A Hybrid Root Finder," *Integral Methods in Science and Engineering*, edited by E. Bertram, C. Constanda, and A. Struthers, Champman & Hall/CRC, London, England, U.K., 2000, pp. 41–50.

[8] Beck, J., and Arnold, K., *Parameter Estimation*, Wiley, New York, 1977.

[9] Avallone, E., and Baumeister, T., *Marks Standard Handbook for Mechanical Engineering*, 10th ed., McGraw–Hill, New York, 1996.

[10] Kreith, F., *CRC Handbook of Thermal Engineering*, CRC Press, New York, 2000.

[§]Information on thermal conductivity of carbon black can be found at http://www.cabot-corp.com/cws/faqbase.nsf/CWSID/cwsFAQ01182001031038PM180?OpenDocument